



Network for Observation of Volcanic and Atmospheric Change (NOVAC)—A global network for volcanic gas monitoring: Network layout and instrument description

Bo Galle,¹ Mattias Johansson,¹ Claudia Rivera,¹ Yan Zhang,¹ Manne Kihlman,² Christoph Kern,³ Thomas Lehmann,³ Ulrich Platt,³ Santiago Arellano,^{1,4} and Silvana Hidalgo⁴

Received 28 January 2009; revised 7 May 2009; accepted 1 September 2009; published 11 March 2010.

[1] This paper presents the global project Network for Observation of Volcanic and Atmospheric Change (NOVAC), the aim of which is automatic gas emission monitoring at active volcanoes worldwide. Data from the network will be used primarily for volcanic risk assessment but also for geophysical research, studies of atmospheric change, and ground validation of satellite instruments. A novel type of instrument, the scanning miniaturized differential optical absorption spectroscopy (Mini-DOAS) instrument, is applied in the network to measure volcanic gas emissions by UV absorption spectroscopy. The instrument is set up 5–10 km downwind of the volcano under study, and typically two to four instruments are deployed at each volcano in order to cover different wind directions and to facilitate measurements of plume height and plume direction. Two different versions of the instrument have been developed. Version I was designed to be a robust and simple instrument for measurement of volcanic SO₂ emissions at high time resolution with minimal power consumption. Version II was designed to allow the best possible spectroscopy and enhanced flexibility in regard to measurement geometry at the cost of larger complexity, power consumption, and price. In this paper the project is described, as well as the developed software, the hardware of the two instrument versions, measurement strategies, data communication, and archiving routines. As of April 2009 a total of 46 instruments have been installed at 18 volcanoes worldwide. As a typical example, the installation at Tungurahua volcano in Ecuador is described, together with some results from the first 21 months of operation at this volcano.

Citation: Galle, B., M. Johansson, C. Rivera, Y. Zhang, M. Kihlman, C. Kern, T. Lehmann, U. Platt, S. Arellano, and S. Hidalgo (2010), Network for Observation of Volcanic and Atmospheric Change (NOVAC)—A global network for volcanic gas monitoring: Network layout and instrument description, *J. Geophys. Res.*, 115, D05304, doi:10.1029/2009JD011823.

1. Introduction

[2] Many different instruments and measurement techniques are used to study volcanic phenomena, such as seismic activity, geochemical changes, and ground deformation. Indicating the storage and release of volatiles from magmas, volcanic gas emission is among the parameters used to understand and forecast volcanic activity.

[3] In particular, high temporal resolution SO₂ emission monitoring over long time scales can provide insight into the presence, volume, and ascent/descent rate of magma bodies prior to, during, and after eruptions [Symonds *et al.*,

1994]. Combined with other geophysical data sets, SO₂ gas time series can help one to understand the dynamics of magma ascent [Sparks, 2003] and their relationship with conduit and hydrothermal processes [Olmos *et al.*, 2007; Arellano *et al.*, 2008; Edmonds *et al.*, 2003a]. The emitted volcanic gases have a large environmental impact on local [Baxter, 1990; Delmelle *et al.*, 2002], regional, and global scales [Halmer *et al.*, 2002; Robock, 2002; Intergovernmental Panel on Climate Change, 2007].

[4] Since its introduction in the 1970s the mask correlation spectrometer (COSPEC) [Moffat and Millan, 1971] has been one of the most important tools for monitoring volcanic gas emissions [Hoff and Millan, 1981; Hoff, 1992]. Differential optical absorption spectroscopy (DOAS) is an increasingly important tool in atmospheric research and monitoring. Since its introduction in the 1970s, active DOAS, using artificial light sources, has been applied for the monitoring of a large number of trace gases, such as NO₂, NO, HCHO, SO₂, O₃, CS₂, and many aromatic hydrocarbons [Platt *et al.*, 1979; Stutz and Platt, 1996;

¹Department of Radio and Space Science, Chalmers University of Technology, Gothenburg, Sweden.

²Kihlman EI och Data Utveckling, Gothenburg, Sweden.

³Institute for Environmental Physics, University of Heidelberg, Heidelberg, Germany.

⁴Instituto Geofísico de la Escuela Politécnica Nacional, Quito, Ecuador.

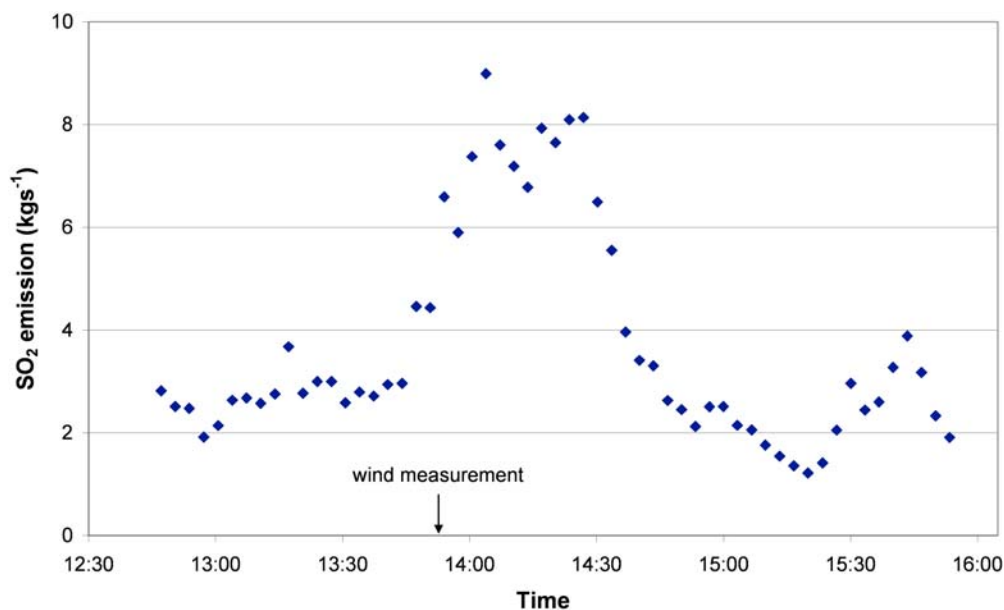


Figure 1. Time-resolved measurement of emissions from San Cristóbal volcano on 23 November 2002.

Volkamer *et al.*, 1998; Yu *et al.*, 2004; Hartl *et al.*, 2006; Kern, 2009; Kern *et al.*, 2009a, 2009b]. Instruments using scattered sunlight from the zenith sky have played an important role in stratospheric research [Noxon, 1975], and the more recent Multi-Axis DOAS (MAX-DOAS) has been successfully applied in tropospheric research [Hönninger and Platt, 2002; Hönninger *et al.*, 2004; Heckel *et al.*, 2005]. Passive DOAS spectroscopy has also recently been applied successfully in volcanic gas monitoring [e.g., Galle *et al.*, 2003; Bobrowski *et al.*, 2003; Edmonds *et al.*, 2003b].

[5] The scanning DOAS instrument uses scattered sunlight in the UV region to derive path-integrated concentrations (columns) of, for example, SO₂, NO₂, BrO, or HCHO using the DOAS technique. The instrument's viewing direction can be changed to any direction in a vertical plane [Edmonds *et al.*, 2003b] or on a conical surface [Galle, 2007] By situating the instrument so that this plane or cone intersects a gas plume, the total number of molecules in a cross section of the plume can be determined, and if the plume velocity is known, the flux through the cross section can be calculated.

[6] Figure 1 shows a time-resolved measurement of the gas emissions from San Cristóbal volcano in Nicaragua using a scanning miniaturized differential optical absorption spectroscopy (Mini-DOAS) instrument. A threefold increase in gas emission is seen over a time scale of 1 hour. Further studies of the gas emission from this volcano using the scanning Mini-DOAS system have revealed cyclic degassing over the course of the day. Correlating these gas data with other geophysical data (e.g., seismic data) is likely to substantially increase our understanding of the status and behavior of this volcano.

[7] The 4 year European Union (EU) funded project Network for Observation of Volcanic and Atmospheric Change (NOVAC) was started in 2005 with the goal of increasing our knowledge of degassing volcanoes, the main

emphasis being on risk assessment. The project aims at establishing a global network of gas observation stations on more than 20 volcanoes by carrying out quantitative measurements of volcanic gas emissions using the scanning DOAS technique.

[8] There are other existing gas-monitoring networks on a few active volcanoes worldwide. On Soufrière Hills volcano on Montserrat, two scanning Mini-DOAS instruments were installed in 2003 [Edmonds *et al.*, 2003b]. Identical instruments were installed at Tungurahua volcano in Ecuador in 2004 [Arellano *et al.*, 2008]. These systems have no onboard processing of data in the instruments. Data are transferred in real time to the observatories, using serial radiomodems, and spectra are processed in an off-line procedure. Scanning Mini-DOAS networks have also been deployed at Stromboli (four instruments) [Burton *et al.*, 2004] and Etna (six instruments) in Italy [Salerno *et al.*, 2006]. These systems use a slightly different design and have an integrated PC. Spectra are evaluated in real time and stored in the instrument's PC, while evaluated data are sent to the observatory using global system for mobile communications (GSM) modems.

2. The NOVAC Project

[9] The idea of the NOVAC project (www.novac-project.eu) is to establish a global network of stations for the quantitative measurement of volcanic gas emissions by UV absorption spectroscopy making use of a novel type of instrument, the scanning dual-beam Mini-DOAS developed within the EU project Development of Optical Remote Sensing Instruments for Volcanological Applications (DORSIVA) [Galle *et al.*, 2006]. The instruments are primarily used to provide new parameters in the toolbox of the observatories for risk assessment, gas emission estimates, and geophysical research on the local scale. However, the extent of the network also enables other



Figure 2. Geographical location of the volcanoes involved in the NOVAC project as of April 2009. The project is open to participation by any interested institution, so the network may be expanded in the future. Also see Table 1. (© Google 2009 and Europa Technologies 2009.)

scientific uses of the data, such as global estimates of volcanic gas emissions, large-scale volcanic correlations, studies of climate change, studies of stratospheric ozone depletion, and, for the first time, large-scale validation of satellite instruments studying volcanic gas emissions.

[10] The scanning dual-beam Mini-DOAS instrument represents a major breakthrough in volcanic gas monitoring. It is capable of performing real-time automatic, unattended measurement of the emission of SO_2 and BrO from a volcano with less than 5 min time resolution during daylight. The high time resolution of the data enables correlations with other geophysical data, thus significantly extending the information available for real-time risk assessment and research at the volcano. By comparing high time resolution gas emission data with emissions from neighboring volcanoes on different geographical scales, or with other geophysical events (earthquakes or tidal waves), mechanisms of volcanic forcing may be revealed.

[11] In addition to the main goal of quantifying volcanic SO_2 emissions, several supplementary science tasks are also being pursued. One of these is to measure species other than SO_2 in the volcanic plumes, such as BrO, ClO, OCIO, and NO_2 . Ongoing work within the NOVAC project has also proven the ability to derive information about the aerosol load in a given volcanic plume directly from measured DOAS spectra [Kern *et al.*, 2009a]. The instruments can also be used to measure background tropospheric composition [e.g., Hönninger *et al.*, 2004; Sinreich *et al.*, 2005] or to derive information on atmospheric aerosols [Wagner *et al.*, 2004; Friess *et al.*, 2006] when installed in remote locations, or to quantify anthropogenic pollution when installed close to urban areas (e.g., Popocatepetl, Mexico [see Kern, 2009]). By, for example, looking toward the zenith during sunrise and sunset, the instruments are also able to measure stratospheric constituents such as NO_2 and O_3 and can therefore in some cases be used to monitor stratospheric conditions [see, e.g., Solomon *et al.*, 1987]. Several global networks using these techniques for global atmospheric

studies related to stratospheric ozone depletion (Network for Detection of Atmospheric Composition Change, NDACC) and climate change (Inter-American Network for Atmospheric/Biospheric Studies, IANABIS) are already established or presently under development. There is a need to complement these networks, especially in the Southern Hemisphere and the tropics, where many active volcanoes are found. One ambition of the NOVAC network, besides the volcano monitoring, is to provide atmospheric data from these regions.

[12] While spectroscopic measurements conducted from satellite platforms have the large advantage of achieving global coverage on the order of days, the major challenge of spaceborne measurements is an accurate quantification of radiative transfer. Especially for volcanic plumes located in the planetary boundary layer or lower regions of the free troposphere, only a fraction of the measured radiation has passed through the area of interest. Therefore the measurement sensitivity is limited, and uncertainties can be large. Ground-based spectroscopic measurements are ideal for validation of satellite data retrievals. The measurement output in both cases is the vertical column density, or the concentration integrated over a vertical path through the plume. While radiative transfer effects also influence the ground-based DOAS instruments [Kern *et al.*, 2009a], the geometry is less susceptible to error, because the instruments are much closer to the plume and the light source (scattered solar radiation) is largely located behind the plume. It is thought that the availability of ground-based DOAS measurements at a large number of volcanoes worldwide with a wide range of emission altitudes, local meteorology, and ground albedo will bring the observation of volcanic gas emissions from space a significant step forward.

[13] The network initially comprised 20 volcanoes in Africa, Europe, South America, and Central America, with funding from the European Commission. During the project an additional four volcanoes have been added, funded from other sources. The network, as of April 2009, is given in the

Table 1. List of Volcanoes Involved in the NOVAC Project as of April 2009

Volcano	Country	Latitude (deg north)	Longitude (deg east)	Summit Elevation (m)	Data Acquired Since	Number of Instruments	
						Version I	Version II
Arenal	Costa Rica	10.463	−84.703	1670	To be installed		
Cotopaxi	Ecuador	−0.677	−78.436	5911	Oct 2007	1	
Colima	Mexico	19.514	−103.62	3850	Dec 2007	2	
Fuego	Guatemala	14.473	−90.880	3763	Apr 2008	2	
Galeras	Colombia	1.22	−77.37	4276	Nov 2007	3	
Kilauea	USA	19.421	−155.287	1222	To be installed		
La Soufrière	Guadeloupe	16.05	−61.67	1467	To be installed		
Llaima	Chile	−38.692	−71.729	3125	To be installed		
Masaya	Nicaragua	11.984	−86.161	635	Apr 2007	2	
Mount Etna	Italy	37.734	15.004	3330	Jul 2008	2	2
Nevado del Huila	Colombia	2.93	−76.03	5364	Apr 2009	2	
Nevado del Ruiz	Colombia	4.895	−75.322	5321	To be installed		
Nyamuragira	D. R. Congo	−1.408	29.20	3058	To be installed		
Nyiragongo	D. R. Congo	−1.52	29.25	3470	Jun 2007	4	
Piton de la Fournaise	Reunion (France)	−21.231	55.713	2632	Aug 2007	3	1
Popocatepetl	Mexico	19.023	−98.622	5426	May 2007	3	1
San Cristóbal	Nicaragua	12.702	−87.004	1745	Nov 2006	3	
San Miguel	El Salvador	13.434	−88.269	2130	Apr 2008	2	
Santa Ana	El Salvador	13.853	−89.630	2381	Apr 2008	2	
Santiaguito	Guatemala	14.739	−91.568	2500	Apr 2008	2	
Tungurahua	Ecuador	−1.467	−78.442	5023	Mar 2007	3	1
Turrialba	Costa Rica	10.025	−83.767	3340	Apr 2008	4	
Villarrica	Chile	−39.422	−72.929	2847	Apr 2009		
Vulcano	Italy	38.404	14.962	500	May 2008	1	

map in Figure 2 as well as in Table 1. More partners are welcome to join.

3. Measurement Strategies

3.1. Scanning Modes

[14] The NOVAC measurement strategy is based on the scanning Mini-DOAS instrument, which collects scattered sunlight and scans the sky over 180°, from horizon to horizon from a location several kilometers downwind of the volcano. From the recorded spectra, integrated trace gas densities per unit length of plume are derived by using the well-established DOAS technique.

[15] In the most commonly used measurement strategy, the instrument scans a vertical plane perpendicular to the anticipated transport direction of the plume (see Figure 3a, plume P1, and Figure 4a). When the plume is above the instrument, the measurement is straightforward. As the wind direction changes, the plume is seen closer to the horizon, and flux errors increase rapidly when the plume gets so low that a clean atmosphere can no longer be seen below the plume, resulting in an incomplete plume. At longer distances between instrument and plume-intersection signal, dilution by scattering also strongly affects the accuracy of the measurements (this and other radiative transfer effects are discussed in detail by Kern *et al.* [2009a]). By implementing a new measurement geometry, where the plume is scanned along a conical surface rather than along a flat vertical surface, these problems are significantly reduced (see Figure 3b) [Johansson, 2008].

[16] With the conical scanning geometry the plume is, for the same plume directions, seen significantly closer to the zenith and at shorter distances from the instrument (see Figure 3). Thus, by using conical scanning geometries, each instrument can manage much larger variations in plume

direction than with simple flat scanning geometries. Thereby, fewer instruments are needed to cover the expected range of wind directions. Figure 4a shows an example of an installation using two flat scanners, and Figure 4b shows the same situation using two conical scanners. It is clear from Figure 4 that the conical scanners cover a larger range of wind directions. The concept of using conical scanning geometries has been thoroughly investigated [Galle, 2007; Johansson, 2008].

[17] In addition to the flat or conical geometries that are alternatively available in the NOVAC Version I instrument, a second version of the NOVAC instrument was built that can use arbitrary user-defined scan geometries (see section 5 for technical implementation). While these instruments can be configured in both the simple flat scan and conical geometries for intercomparison with NOVAC Version I instruments, more advanced geometries are also available. Examples include subsequently using different scanning planes to study the evolution of a volcanic plume or dynamically adjusting the scanning plane to achieve perpendicular intersection with the volcanic plume if possible, thus minimizing errors in the calculation of integrated trace gas densities per unit length of the plume (see section 7 for a detailed error analysis).

3.2. Plume Speed Measurements

[18] One of the major sources of error in both mobile and scanning Mini-DOAS measurements, as well as COSPEC measurements, is determination of wind speed at plume height [Stoiber *et al.*, 1983; Salerno *et al.*, 2009]. To reduce this error, a novel technique for measuring the speed of the plume using a modified version of the Mini-DOAS instrument has been developed in the DORSIVA project [Johansson *et al.*, 2009a]: the dual-beam instrument. The modified instrument contains two spectrometers, coupled to

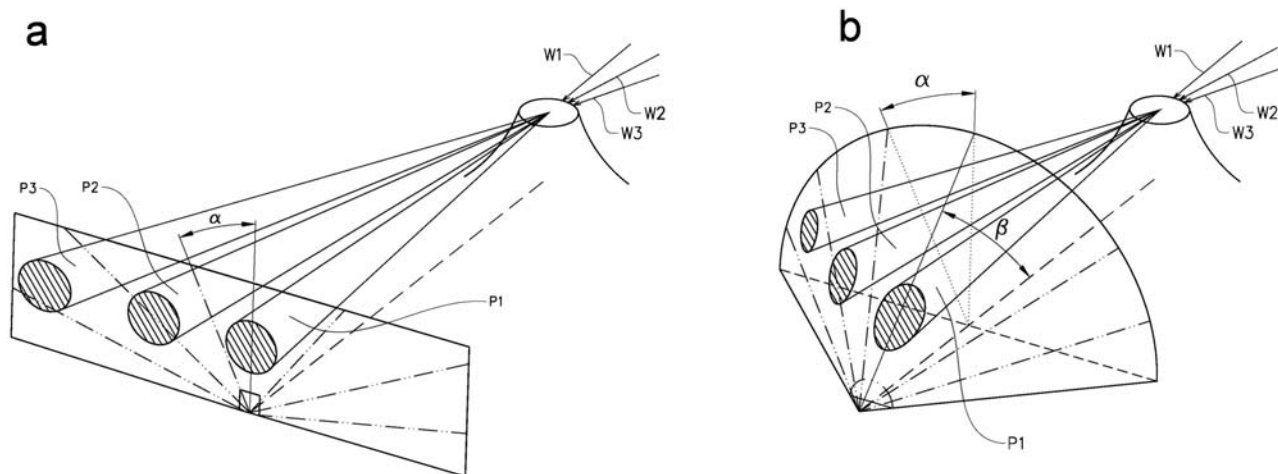


Figure 3. Different scan geometries for volcanic gas emission measurements: (a) flat scanning geometry and (b) conical scanning geometry, where α is scan angle and β is cone opening angle.

the telescope with fibers in such a way that the fields of view of the two spectrometers are separated by a small angle, typically 80 mrad. Wind measurements are made by pointing both fields of view toward the center of the plume at different distances downwind of the volcanic vent (Figure 5). If the plume height is known (see section 3.3), the horizontal distance between both intersections of the instrument fields of view with the plume can be calculated. A time series of total column variations is registered in both directions, and from the temporal delay in variations in the total column, combined with the distance between the intersection points, the wind speed can be derived. Ideally, the parameter to be measured is the wind speed at plume height, weighted by plume concentration. As this approach uses variations in the total column of SO_2 to determine the plume speed, a weighting with concentration is automatically made. These measurements can be performed using the Version I instrument with flat scanning geometry. Measurements can also be performed using the Version I instrument with conical scanning geometry; however, this requires that the cone axis of the scanner is tilted to enable the instrument to view the zenith. In the Version II instrument, wind speed may be measured in a similar manner by sequentially collecting column data from two different directions (see Kern [2009] for examples).

3.3. Plume Height, Direction, and Tomography

[19] For an accurate determination of volcanic gas emissions using scanning Mini-DOAS instruments, knowledge of the plume height and plume direction is important (see section 3.2 and Edmonds *et al.* [2003b]). These parameters can be derived if the gas plume is viewed simultaneously by two scanning Mini-DOAS instruments separated by some distance [Edmonds *et al.*, 2003b].

[20] The height and direction of the plume can be calculated by combining two scans from spatially separated instruments (see Figure 6). The calculation is performed as follows: for each of the two scans the measurement direction corresponding to the center of mass of the plume is determined, and lines originating in the instrument (Γ_1 and Γ_2) are constructed in these directions. By using an initial assumption of the plume height (h_0), these two lines are

used to calculate two plume propagation directions of the plume by first calculating the interception points (p_1 and p_2) between each of the lines Γ_1 and Γ_2 and an imagined plane at altitude h_0 and then calculating the direction of the line from the emission source to each of the two points p_1 and p_2 . If the assumed plume height differs from the true plume height, then these two directions will differ. An iterative Gauss-Newton search is then performed in which the assumed plume height h is updated in each step. The search is considered to have converged when the assumed plume height yields two plume directions that differ by less than one degree, giving an estimate of the height and direction of the plume. This algorithm was selected because it is fairly robust and does allow for different scanning geometries of the two instruments used.

[21] Under favorable conditions, the gas concentration in a vertical cross section of the plume can be derived using tomography [Johansson *et al.*, 2009b; Wright *et al.*, 2008; Kazahaya *et al.*, 2008]. These data can be used to study the plume dynamics and, in combination with a dispersion

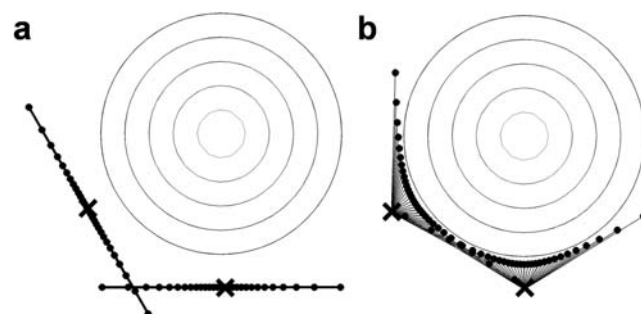


Figure 4. Examples of different scan geometries for measurements of volcanic gas emissions. (a) A measurement setup using two flat scanners and (b) a measurement setup using two conical scanners. The view is from above, showing the idealized volcano as altitude curves, the interception points between the instruments viewing directions and an imagined plane at the altitude of the plume as dots, and the instrument positions as crosses.

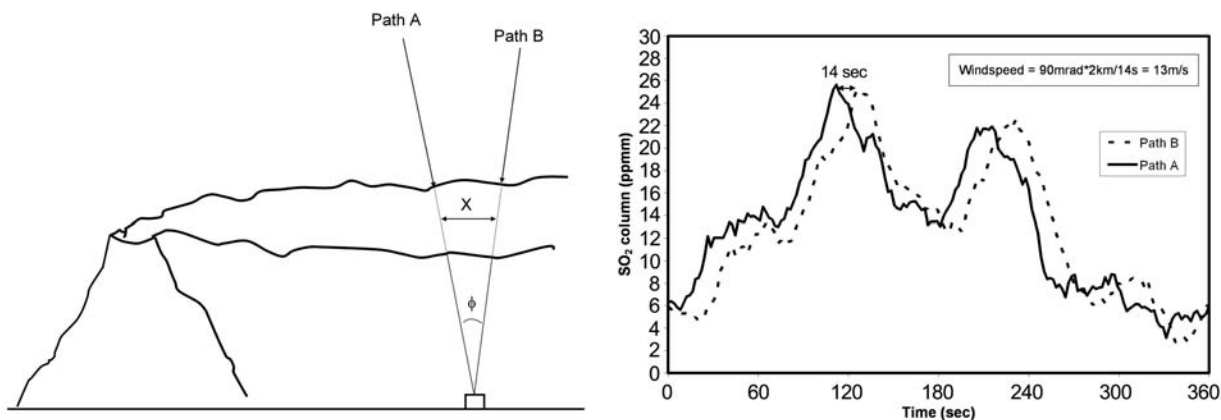


Figure 5. (left) The speed of the plume can be determined by collecting two time series of column data, one farther upwind than the other. (right) Measurement of the speed of the SO₂ plume from San Cristóbal volcano, Nicaragua [Galle et al., 2006].

model, to assess the impact of the gas emissions on the local environment.

4. Network Layout

4.1. General Considerations

[22] Deployment of automatic instruments at active volcanoes poses a number of challenges. Many volcanoes are located in remote places with limited infrastructure. A tropical climate adds technical difficulties related to high and strongly varying temperatures, high humidity, and heavy rainfall. In addition, the chemical environment downwind of an active volcano involves highly corrosive gases, acid rain, and ashfall. Thus the following issues need to be taken into account in the instrument and network design.

[23] 1. Few volcanoes can provide reliable electric power for the instruments. In case of a volcanic crisis, even the most robust electric power network is likely to fail. Thus the

instruments have to rely on solar power, have low power consumption, and be able to operate on 12 V. Power-saving modes such as turnoff at night and low standby power should be applied.

[24] 2. For data communication the consequences of a volcanic crisis need to be considered. Real-time transmission using ground-based communication links is likely to fail. Satellite communication or the use of GSM networks is more robust; however, GSM networks have limited coverage at volcanic sites, and both options get expensive if large data sets are transmitted. The compromise chosen for the NOVAC project is to use ground-based wireless transmission of real-time data, complemented by buffering of data in the instrument in case of network failure.

[25] 3. For the instrument hardware, industry- or military-grade components have been chosen, and care has been taken to minimize the number of moving components as well as, whenever possible, the use of noncorrosive material

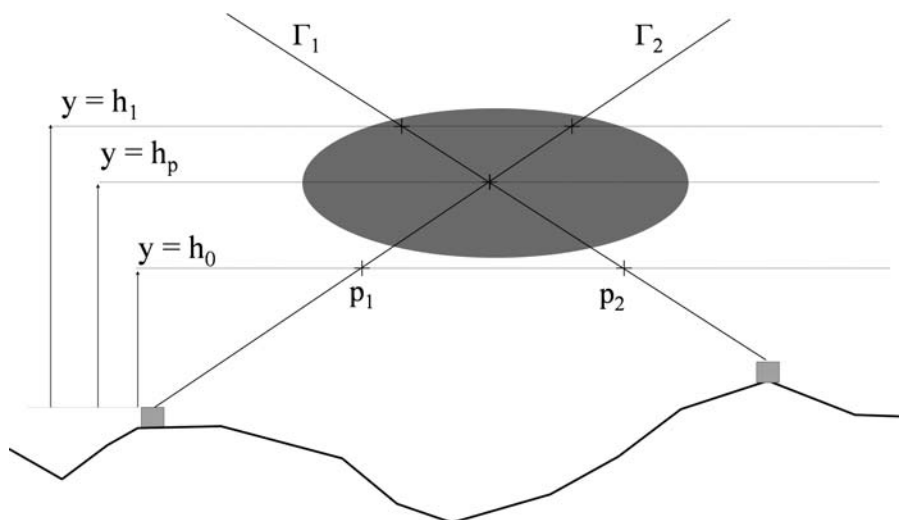


Figure 6. The altitude of the gas plume can be determined if two scanning instruments see the plume simultaneously. First a line is drawn from each of the instruments in the direction of the center of the plume. Then a plume height is assumed, and for each of the instruments, the wind direction is calculated under the assumed plume height. When the assumed plume height equals the true plume height, the two calculations give the same wind direction.

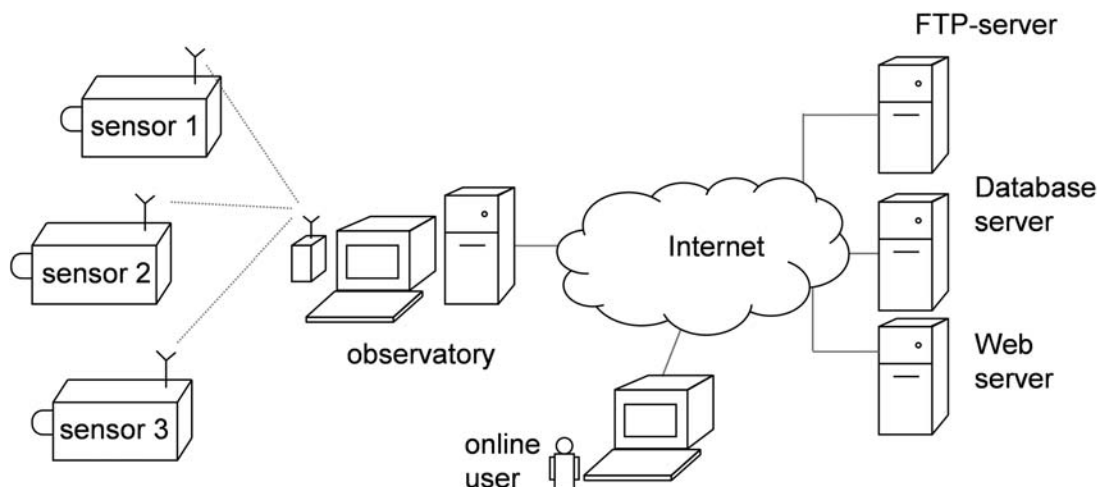


Figure 7. Network architecture. The data collected by the instruments are downloaded to a computer in the observatory by the observatory software. The software evaluates the data for SO_2 and calculates the SO_2 flux. The spectra, evaluated results, and calculated fluxes are then uploaded to the central database servers from where they are accessible to the participants of the project.

such as plastic and stainless steel. By making it possible to separate the scanning unit from the spectrometer and electronics, the latter more sensitive components can be located in a less exposed place, for example, inside an existing building or in a sealed box underground if necessary.

[26] 4. Security is an issue because the remote location of the instruments makes them exposed to the risk of theft or vandalism. By careful choice of sites and special design of the supporting platform for the instrument components, these risks can be minimized.

[27] 5. The instruments are often placed in open areas at high altitudes, which makes them subject to lightning. This problem can be minimized by careful choice of the sites as well as proper grounding of masts and antennas.

[28] 6. As many of the instruments are located in remote and inaccessible locations, strong efforts should be made to minimize maintenance needs through automation.

4.2. Communication System

[29] The global network includes instruments, local servers, and central servers. The instruments collect and store spectra autonomously. Upon request from the management software (see section 6) running in the local observatory, the spectra are then downloaded to the local server in the observatory. Once downloaded, the software evaluates the spectra for SO_2 and calculates the flux using the best estimate of wind speed and wind direction available; the software then presents the calculated gas emission in real time. The spectra and the evaluated results are then uploaded to a central server located at Chalmers University in Sweden. Spectra and evaluated results are forwarded to database servers at the University of Heidelberg (UHEI) and at the Belgian Institute for Space Aeronomy (BIRA), from which the scientific data are available to project participants. The network architecture is schematically described in Figure 7.

[30] The network typically contains two to three instruments at each volcano. These instruments are usually located on the slope of the volcano, 20–100 km away from

the volcano observatory. Because of the long distance, building a wired network would be overly expensive. Hence, wireless network is the obvious solution for communication. The basic network structure is point-to-multipoint. In order to make data transmission simple and efficient, no routing protocol is used in the local network.

5. Instrument Hardware

5.1. Instrument Optics

[31] As described in section 2, the main focus of the NOVAC project is the quantification of volcanic SO_2 emissions and the use of these for volcanic risk assessment. In addition to this main goal, several supplementary science tasks are also being pursued, such as studies of other volcanic gases and studies of tropospheric and stratospheric gas composition.

[32] It was found that the instrument requirements for the supplementary science questions deviate from the basic measurement of volcanic SO_2 fluxes. For one, a high time resolution is important for the correct assessment of fluxes, because the temporal variability of the flux can be high (see Figure 1). However, for measuring additional trace gas species, a high optical resolution can be advantageous. This typically decreases light throughput and therefore negatively affects time resolution. Energy consumption poses another conflict of interest (see section 4.1). In many cases, power is extremely limited and supplied only by solar panels. There are some situations, however, in which additional power is available, either because a landline is accessible or because the NOVAC instrument was colocated with a large monitoring station with accordingly dimensioned solar panels and batteries. In such cases, it is possible to actively regulate the temperature of the NOVAC spectrometer, which has been found to greatly reduce calibration shifts and changes in the optical transfer function, thus enhancing the quality of the spectroscopy. Lastly, while the conical geometry (see section 3.1) is well suited for measuring SO_2 fluxes for a large range of wind directions, it is not ideal for tropospheric and stratospheric background measurements. For these,

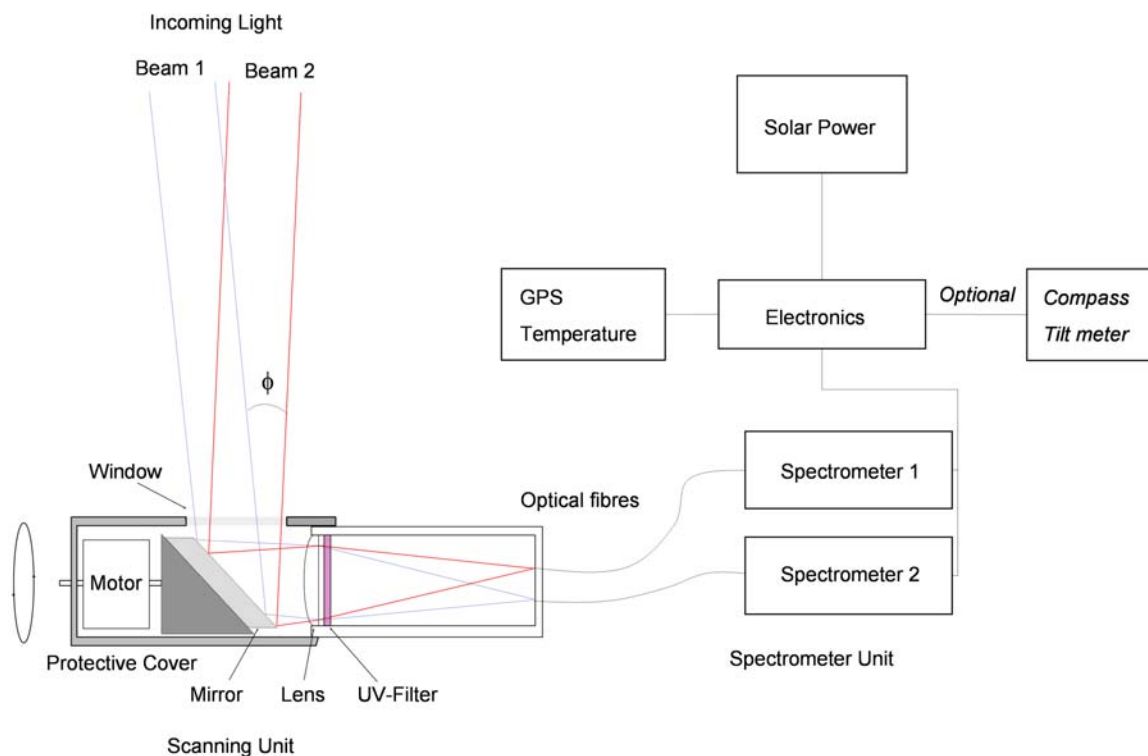


Figure 8. Schematic view of the NOVAC Version I instrument.

additional flexibility in regard to the instrument viewing direction is desirable. Owing to these irreconcilable demands and the desire to maximize the scientific output of the deployed instruments, two separate optical configurations were designed and employed according to individual installation conditions and science goals. Both are described in the following.

5.1.1. Version I Optics

[33] The NOVAC Version I instrument was designed to be a robust and simple instrument for measurement of volcanic SO_2 emission fluxes at high time resolution with minimal power consumption. The instrument consists of a pointing telescope fiber-coupled to an S2000 spectrometer from Ocean Optics Inc. Ultraviolet light from the Sun, scattered by aerosols and molecules in the atmosphere, is collected by means of a telescope with a quartz lens defining a field of view of 8 mrad. The telescope is attached to a scanning device consisting of a mirror mounted on a computer-controlled stepper motor, providing a means to scan the field of view of the instrument over 180° (Figure 8). The collected light is transferred from the telescope to the spectrometer through an optical quartz fiber. The spectrometer uses a 2400 lines/mm grating, which when combined with a $50 \mu\text{m}$ slit, provides an optical resolution of $\sim 0.6 \text{ nm}$ over the wavelength range of 280–420 nm. A band-pass filter (Hoya U330), blocking visible light with wavelength longer than 360 nm, is installed in the telescope $\sim 2 \text{ mm}$ behind the lens, with the purpose of reducing spectrometer stray light.

[34] In an ideal measurement, the instrument is located under the plume, and scans are made, from horizon to horizon, in a vertical plane or along a conical surface approximately perpendicular to the wind direction. Typically,

a 3 s integration time is used with a spectrum collected every 3.6° , providing a full flux measurement every 5 min. By adding a second spectrometer (Ocean Optics Inc. SD2000) and fiber and by separating the fibers by 6 mm at the focal plane of the telescope (see Figure 8), simultaneous measurements can be made in two viewing directions separated by 80 mrad, constituting the scanning dual-beam Mini-DOAS and enabling plume speed measurements (see section 3.2).

[35] Figure 9 shows a typical installation of a NOVAC Version I instrument. The scanning unit is mounted on top of a 3.5 m high pole. The optical fibers and the cable from



Figure 9. NOVAC Version I instrument installed at San Cristóbal volcano, Nicaragua.

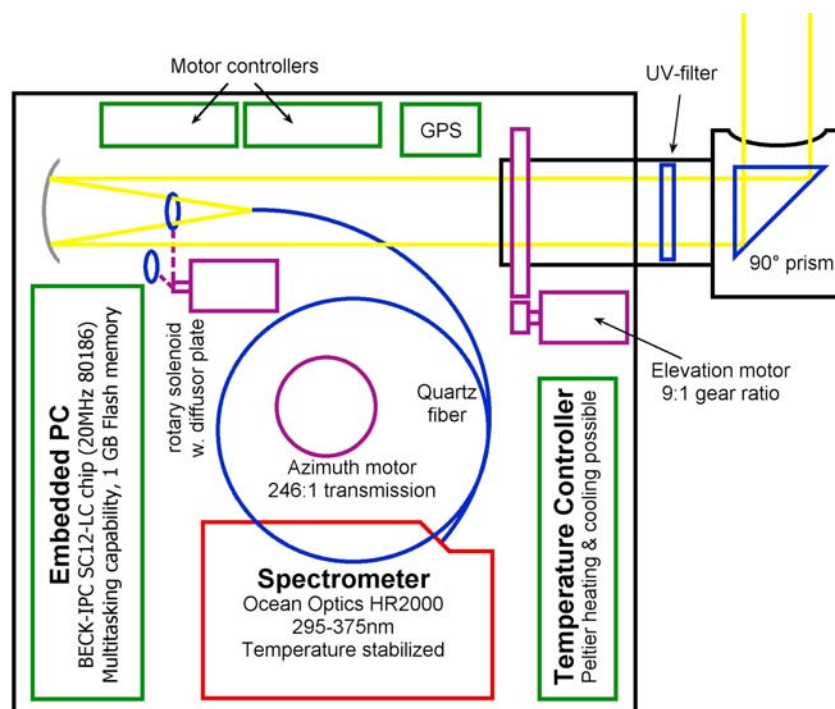


Figure 10. Schematic view of the NOVAC Version II instrument as seen from the top. Light enters the system through the elevation scanner protruding from the side of the instrument. After passing through a UV filter, the light is collimated by a spherical mirror and focused on the end of a fused silica fiber leading to the spectrometer. A diffuser plate can be moved into the light path for solar occultation measurements using a rotary solenoid.

the scanner are fed inside the pole to the instrument box located under the solar panel. The solar panel thus provides shade and protection against rain and dust to the electronics. The battery and regulator for the solar power are located in a separate compartment below the spectrometer and electronics to avoid corrosion from battery gases. Between the scanner and the solar panel, the wireless access point with integrated antenna used for the data communication is seen, pointing toward another wireless access point located at a seismic station on the lower left slope of the volcano. Another example of an installation is shown in Figure 13.

5.1.2. Version II Optics

[36] The NOVAC Version II instrument was designed to allow the best possible spectroscopy and enhanced flexibility in regard to measurement geometry. An improved optical resolution of 0.4 nm is achieved by replacing the Ocean Optics S2000 with an Ocean Optics HR2000 with a focal length of 101.6 mm at $f/4$, a 100 μm entrance slit, and a 2400 groove/mm grating, yielding a wavelength range of 295–390 nm. The spectrometer optical bench temperature is controlled by a thermoelectric Peltier module regulated using a SuperCool PR-59 temperature controller with constant voltage pulse width modulation. To keep power consumption to a minimum, the temperature is typically kept constant at the average daytime ambient temperature at the instrument's location, and the spectrometer is wrapped in Armaflex insulating foam. Both heating and cooling are possible. Excess heat is dissipated by a heat sink located on the underside of the instrument, where it is shielded from the Sun. The thermoelectric temperature regulator can consume up to 50 W in addition to the rest of the electronics

(described in section 5.2), but typical values are much lower, as less than 1 W/ $^{\circ}\text{C}$ is consumed for a given temperature difference between spectrometer and ambient.

[37] The Version II optics feature a dual-axis scanner that allows the instrument to point in any direction in the sky or, as is sometimes useful for tropospheric measurement, at the ground. One scanning element protrudes from the side of the instrument (see Figure 10), while the entire instrument box is mounted on a vertical axis that allows the additional adjustment of the instrument's azimuth angle. Both axes are positioned using Faulhaber brushless DC servomotors with position generators. The motors are controlled by Faulhaber MCBL 3003 motor drivers, which in turn receive their instructions from an embedded PC running the measurement (same as for Version I, described in section 5.2). The elevation and the azimuth scanner motors use gear reductions of 9:1 and 246:1, respectively. The achieved relative position accuracy was found to be better than 0.05° [Sommer, 2008].

[38] Figure 10 shows the optical paths inside the NOVAC Version II optics. Scattered light enters the scanner on the side of the instrument. It is deflected by 90° by a prism which replaces the mirror to avoid variable sensitivity to different directions of polarization. After passing through a Hoya U330 UV filter, the incident light is collimated with a 25 mm diameter spherical mirror and is focused onto a single 400 μm fused silica fiber positioned in the focal point 75 mm away and leading to the spectrometer. Between the mirror and the fiber entrance, a diffuser plate can be moved in and out of the light path with a rotary solenoid for solar occultation measurements. The diffuser plate is thus used to

Table 2. Power Consumption in Watts of the NOVAC Version I Instrument Operated in Different Power Modes

	Electronics	Scanner	GPS		Radio	Total (W)
			Receiver	Spectrometer		
Full operation	2	1	0.5	1.9	1.5	6.9
Reduced stepper current	2	0.2	0.5	1.9	1.5	6.1
Sleep mode	2	0	0.5	0	1.5	4
Timer off	0	0	0	0	0	0

attenuate the incident radiation while at the same time mixing variations in the spectrum originating in different positions on the solar disk (see *Sommer* [2008] for details).

[39] The dimensions of the instrument box are $30 \times 30 \times 15$ cm, and the instrument weighs approximately 7 kg. It can be mounted either on a fixed structure for permanent installation or on a tripod for mobile measurements.

5.2. Instrument Electronics

[40] An embedded PC controls the peripheral components in the sensor, with the assistance of a software package especially developed to control spectra collection, read out information from the GPS receiver and temperature sensor, handle data communication, and manage the file system. The embedded PC is built around the SC12 “System-On-A-Chip” from Beck IPC GmbH, composed of one 186 processor running at 20 MHz, 512 kbytes RAM, 512 kbytes flash Electrically Erasable Programmable Read-Only Memory (EEPROM), 10 Mbit Ethernet, and two serial ports. A multitasking operating system is integrated in the flash EEPROM. It functions with unregulated power at voltages between 10 and 24 V.

[41] The behavior of the instrument, for example, settings of viewing angles and exposure time, is defined in a text file that is uploaded to the embedded PC. Data are stored and handled as files in the standardized File Allocation Table (FAT) format on the PC. In order to run autonomously for a long period of time, a 1 GB Compact Flash card is used to store spectral data. Spectral data are compressed with a data compression algorithm in order to minimize storage size and data-transfer time. The size of a compressed file is ~ 50 – 60% of the raw spectrum from the spectrometer. Spectra are grouped by scans with one scan in each file. A compressed file, containing a typical scan of 53 spectra, has a size of ~ 130 kbytes. Assuming the sensor works 12 h a day and makes one scan in 5 min, the data can be stored for 56 days in a 1 Gbyte Compact Flash card. The memory card can be expanded up to 2 Gbyte, enabling more data to be collected in the instrument.

[42] A GPS receiver is used to give precise position and time tags for all measurements. The embedded PC holds an eight-channel AD converter of which the first channel is used to digitize the battery voltage, and the second channel is used to digitize the temperature of the system as determined by an analog sensor. The remaining six channels on the AD converter are currently unused and free for future extension of the system.

[43] The embedded operating system has network capabilities, including a Web server, an ftp server, and built-in commands for using the network interface. The data in the

Compact Flash can be downloaded through the ftp server installed on the embedded PC. The embedded PC can also work as ftp client and, when connected to the Internet, can be set to automatically upload spectra files to an ftp server. Another way to download data is by a novel serial communication protocol, which sends data in 8 kbyte sized packets and deploys checksums to detect errors in communication.

[44] The system is powered by solar panels in combination with a 12 V battery. Owing to the limitation of power, the system reduces power consumption in three ways. First, the system uses a timer to control operation time. Because the collection of spectra depends on UV light, the system operation time is limited to the hours when there is daylight. The timer automatically switches all the components of the system, including scanner, electronics, spectrometer, and radio, on in the morning and off in the evening. Besides saving power, this operation also makes sure that all systems are reset at least once per day. Second, the system saves power by entering a “sleep” mode about 4 h before the timer power off. During sleep mode, spectrometer and scanner are turned off, while electronics and radio are still on. Third, the system can be set to reduce the stepper motor current when the motor is holding a position as compared to when it is stepping. The power consumption of the NOVAC Version I instrument, assuming use of a FreeWave FGR 115RC transceiver for the external communication, is given in Table 2. The NOVAC Version II instrument has an additional power consumption of 1–50 W, depending on the difference between spectrometer and ambient temperatures and the degree of active temperature stabilization used.

5.3. Communication Hardware

[45] There are many possible solutions for the wireless link from the instruments to the server in the observatory. Wireless access points, radio modem, GSM, general packet radio service (GPRS), and satellite are all possible communication solutions for setting up long-distance links. The required bandwidth is modest, because a typical measurement from one instrument produces 140 kilobytes of data every 6 min. Using a bandwidth of 57 kbps, these data are transferred in ~ 20 s.

[46] A radio modem network is a common solution for data transfer at many volcano observatories, since they can transmit data over long distances with low power consumption. However, the bandwidth is limited (typically 115 kbps), and flexible network topology is not easily applicable. Therefore radio modems are chosen when the network has a simple structure and/or very long transmission ranges are needed. Wireless access points have very broad bandwidth, up to 54 Mbps, but also higher power consumption and shorter range than radio modems. GSM or GPRS may be an option where this infrastructure is available, and satellites are always an attractive solution at remote locations. However, for both these methods the cost per day is considered too high for routine monitoring.

[47] After comparison of these instrument solutions on bandwidth, range, power consumption, reliability, cost, etc., it was decided to use serial radio modems (FreeWave Inc., FGR115-RC, effective baud rate 57 kbps), unless wireless access points were already available at the volcano. For limited campaigns, for example, in connection with a

volcanic crisis or a specific research task, satellite communication is suggested as an alternative solution.

6. Instrument Software

6.1. Observatory Software

[48] To evaluate the data collected by the scanning instruments, a software package called the NovacProgram has been developed. The software is designed to supervise several connected instruments simultaneously and to download data from them, one at a time. The software is intended to run on a desktop computer in the observatory, where it can connect both to the instruments and to the Internet, for uploading of the evaluated data to an ftp server.

[49] The NovacProgram monitors the connected instruments and downloads available data from them. The collected spectra are then automatically evaluated for SO₂, and for each complete scan from horizon to horizon, the SO₂ emission from the volcano is calculated using the best value of wind speed, wind direction, and plume height available. The evaluated SO₂ columns and the calculated fluxes are presented in real time to the user in the observatory via a graphical interface. For each connected NOVAC instrument, the parameters necessary for evaluating the spectra must be provided at the time of installation, as well as parameters for how to connect to the instrument.

[50] To date, the software package is capable of connecting to the scanning instruments in one of three ways: (1) over a direct serial link, such as a serial cable or a pair of serial radiomodems, (2) over a point-to-multipoint network based on serial radiomodems, and (3) over a Transmission Control Protocol/Internet Protocol (TCP/IP) network using the ftp protocol.

[51] In each of these modes, the program sequentially polls the instruments for new data and at the same time checks the status of the instrument. If there are data available for downloading, the program initiates a download of the data. If necessary, the program can also stop the data collection software inside the instrument and turn off the power of the spectrometer, for example, to let the instrument “sleep” over night.

[52] When evaluated, the spectral data are stored in the observatory computer, in the same compressed format as in the instrument, with all spectra from one scan in each file. The name of the file identifies the serial number of the spectrometer that collected it, the date, and the UTC time when the collection of the scan started. Each such spectral file is accompanied by an ASCII text file with the same name, but different file ending, containing the result of the evaluation of the spectra in that scan and the calculated flux. In addition to these, a flux-log file is generated containing the calculated fluxes for one day. The spectral data and the results of the evaluation are then automatically uploaded to a central ftp server.

[53] If two instruments installed on the same volcano can see the plume within a given short time interval, then plume height and wind direction are automatically calculated (see section 3.3 for a description of how this is done) and stored for use in later reprocessing of the data.

[54] If equipped with two spectrometers, the NOVAC-scanning instruments are capable of performing wind speed measurements using the dual-beam technique as described

in section 3.2. If properly configured, the observatory software is capable of initiating wind speed measurements whenever the plume is passing over one instrument and the conditions are good. The judgment is performed by the software by studying the most recent measurements and from these by judging the direction of the plume, the stability of the plume direction, and the strength of the plume. The measurement is started by the uploading of a small command file to the instrument that will perform the measurement.

[55] To enable the user to inspect the collected data more closely and possibly to recalculate the fluxes using updated values of the wind speed, wind direction, and plume height, a postflux calculation dialog has been built into the program. Furthermore, a spectral reevaluation dialog makes it possible to inspect the quality of the spectral evaluation and to evaluate the spectra again using a different set of parameters. Both of these dialogs can also be run in batch mode to facilitate reprocessing of data from one or several days. All the information related to the flux calculation is recorded in the database, including meteorological and geometrical parameters and the source from which they were retrieved.

6.2. Spectroscopy

[56] Collected spectra are processed by the observatory software in real time, deriving a slant column of SO₂ from each spectrum. The derivation is performed through a DOAS fit, in which the Fraunhofer structures are removed by division by a zenith spectrum collected in the beginning of the scan and broadband absorption features are removed by applying a binomial high-pass filter on the absorption spectrum. The short time between the collection of the Fraunhofer spectrum and the other spectra minimizes the effect of wavelength shifts between the Fraunhofer spectrum and the other spectra due to changes in temperature. An example of the fitting of an in-plume spectrum can be seen in Figure 11, where one spectrum collected at Masaya volcano, Nicaragua, on 29 May 2007 is evaluated in the wavelength range 310–325 nm using a differential SO₂ cross section. To compensate for the possibility that the zenith spectrum collected in the beginning of the scan contains absorption by SO₂, an additional parameter, the offset, is introduced. This is defined as the negative of the SO₂ column in the zenith spectrum and is estimated from the scan as the average of the 20% lowest SO₂ columns in the scan. For this estimate to be close to the true SO₂ column in the zenith spectrum, it is necessary that some part of the measurement is performed outside of the plume. This offset is then subtracted from the derived SO₂ column for each measured spectrum before any further calculations can be done.

[57] In the standard procedure the SO₂ columns are derived from the spectra in the wavelength range 310–325 nm using the differential cross sections of SO₂ [Vandaele *et al.*, 1994], O₃ [Voigt *et al.*, 2001], and a Ring spectrum calculated using the DOASIS software (DOASIS, version 3.2.2734, programmed by S. Kraus, available at <http://www.iup.uni-heidelberg.de/bugtracker/projects/doasis/>). The fitting procedure is implemented using the nonlinear least squares fit routines from the DOASIS software.

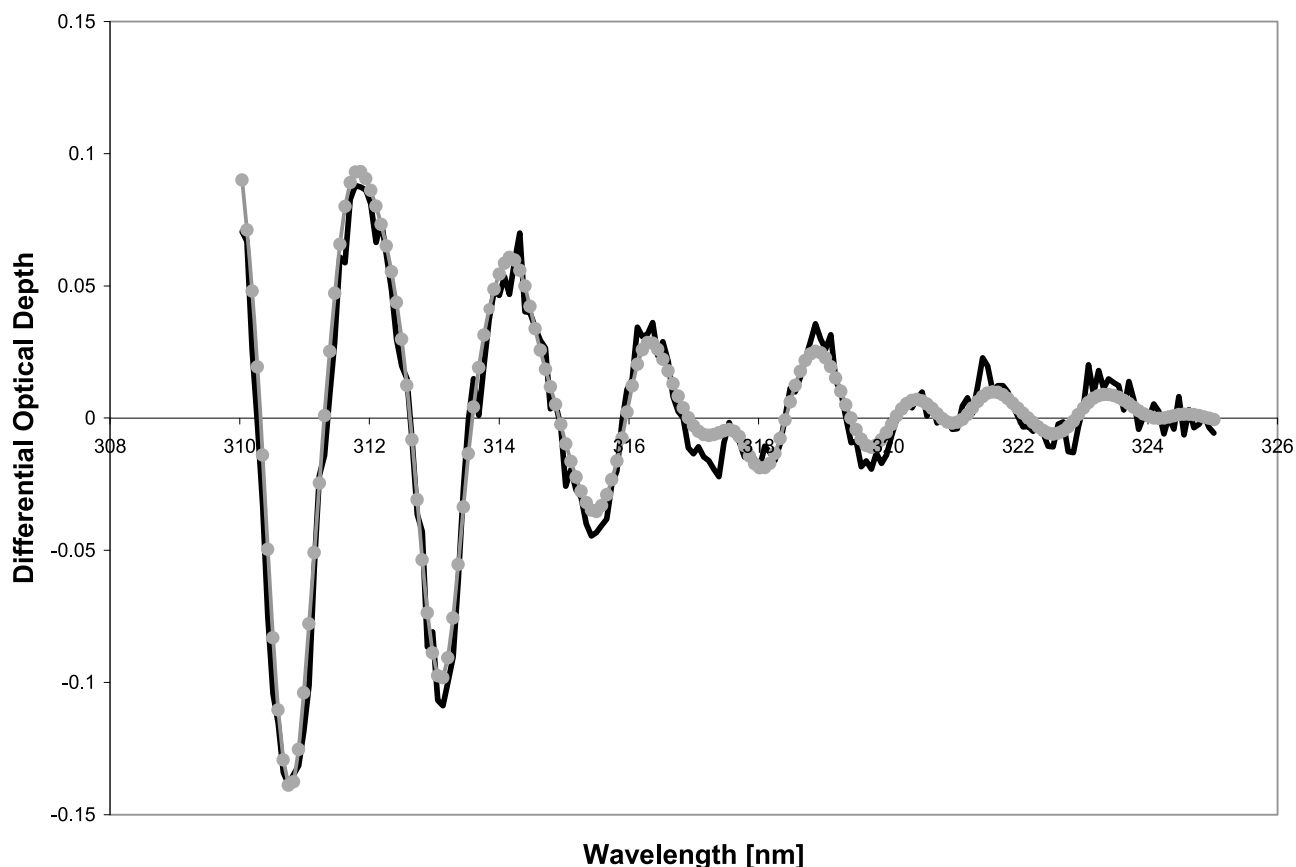


Figure 11. Example of an SO₂ fit from a spectrum collected in a volcanic plume at Masaya volcano, Nicaragua, on 29 May 2007. Solid line shows measured spectrum, and dotted line shows fitted differential SO₂ cross section. Evaluated SO₂ column is 1.90×10^{18} molecules/cm² (286 mg/m²).

[58] Some of the problems with the COSPEC instrument are limited sensitivity, poor linearity, interferences from other gases and solar Fraunhofer lines, and effects due to multiple scattering and polarization in aerosol layers and clouds. During the past decade, significant improvements in radiative transfer modeling and the understanding of multiple scattering processes in the atmosphere have been achieved. *Wagner et al.* [2004] and *Friess et al.* [2006], for example, describe techniques for retrieving information on optical paths in the atmosphere from the measurement of the oxygen dimmer O₄, which has a known concentration profile in the atmosphere. As the NOVAC instruments register a broadband spectrum, this also gives one an opportunity to significantly improve the sensitivity and reliability of the above mentioned measurement strategies as well as to expand it to more compounds. An example of this is the possibility of simultaneously deriving SO₂ and BrO from volcanic gas spectra [*Bobrowski et al.*, 2003]. This opens up the possibility of making time-resolved measurements of the ratio BrO/SO₂, another parameter that may be used to understand volcanic degassing and eruptive style. In addition, the universal nature of the instrument recording spectral information in more than 2000 channels allows the monitoring of further species (e.g., CS₂ or OCIO) in the future.

[59] The NOVAC instruments record scattered sunlight spectra in a wavelength band that has previously been used for studies of atmospheric gas composition. Examples

include studies of stratospheric gas composition (e.g., O₃, NO₂, and BrO) and the recently developed technique of MAX-DOAS for studies of tropospheric gases (e.g., SO₂, O₃, NO₂, and HCHO) [*Hönninger et al.*, 2004].

6.3. Data Archiving

[60] Owing to the large number of continuous measurements conducted in the scope of the NOVAC project, it was necessary to implement a fast, user-friendly database that allows access to all the collected data. Online since the middle of 2006, the NOVAC database is structured in such a manner that searching for and accessing the measurement data is as versatile and clear as possible and takes into account that project members use the database in a variety of different ways. Technicians check on instrument functionality, volcanologists are interested in the evaluated emission data, and scientists with backgrounds in spectroscopy can use the raw data to verify retrievals and possibly evaluate additional volcanic and atmospheric parameters. Therefore the data were structured in layers, the top of which contains basic information about each instrument. The second layer contains evaluated emission data, while the bottom layer contains raw data in the form of all spectra measured by the instruments. Complex search and sort functionality is implemented on a layer basis for all data layers.

[61] A robust structure and modular programming are important to allow later changes and scalability. Because of

the expected extent of the data set, major emphasis was placed on performance optimization. At project completion, the database will contain measurement data from at least 24 volcanoes and shall be scalable for up to 200 or more. As the data set grows, performance will be monitored and optimized. Also, the hardware will be continuously upgraded to meet data storage and computing power needs.

[62] The data are stored in six different tables implemented in MySQL (version 5.1, available at <http://www.mysql.com>), which are connected to ensure referential integrity. Storing and querying the data are done with PHP (PHP Hypertext Preprocessor) functions. The system runs in both Linux and Windows environments. A Web interface with over 130 different search, display, and sorting options serves as the user interface and allows sophisticated data access. Each user has a separate account and can save his personal search configuration from session to session. Search results are displayed in table form and can be downloaded by the user. This includes the measured spectra themselves. All in all, the NOVAC database represents a very powerful tool and is crucial for optimal access and exploitation of the immense data set collected during the course of the project. As of December 2008, more than 24 million spectra have been stored in the archive.

7. Error Analysis

[63] The error in the flux measurement is a combination of the errors related to spectroscopy, measurement geometry, atmospheric scattering, and wind parameters. The spectroscopy errors are instrument-dependent and may be quantified in detailed experiments, while the remaining most important errors are strongly dependent on the local measurement geometry and meteorological conditions. Significant efforts are being made to quantify all these errors under different geographical and meteorological conditions. A qualitative description of the different errors followed by error estimates based on current experience will be given here. A more rigorous treatment of each of the error sources will be published in future papers.

7.1. Spectroscopy Related Error

[64] The error related to spectroscopy involves errors in absorption cross section, nonlinear absorption, stray light in the spectrometer, and temperature dependence in slit function and wavelength calibration. The errors in absorption cross section and nonlinear behavior in Beer's law are well documented and can be modeled, while the major spectroscopic errors from stray light and temperature effects are individual to each spectrometer. In the current instrument concept, stray light is reduced by means of a filter (Hoya U330). In addition, the first-order offset in the spectra is subtracted in the evaluation procedure. In the NOVAC Version II instrument, the temperature effects are minimized by active temperature stabilization of the spectrometer. In the Version I instrument, power consumption is minimized, and thus no active temperature control is implemented. Instead, passive temperature stabilization is obtained by separating the scanner unit from the spectrometer and electronics and by locating the spectrometer and electronics in a more temperature stable environment (e.g., inside a

building or in a box below ground). Further details on the possible errors associated with imperfect spectroscopy of SO₂ are given by Kern [2009].

7.2. Measurement Geometry Related Error

[65] With the applied measurement geometries, the evaluation of the integrated number of molecules over the plume cross section involves knowledge of plume height. Ideally, the two-dimensional distribution of concentration over the scanned surface should be known. This may, under favorable conditions, be achieved using tomographic techniques if the plume is simultaneously viewed by two scanning instruments located some distance apart (see section 3.3). Under routine conditions, it is more realistic to get an average plume height from the angular position of the center of mass of the plume as seen by the two systems. The plume height may also be modeled by a meteorological mesoscale model or visually estimated. Additional geometrical errors are caused by deviation between real and idealized geometry of the plume dispersion, projection errors, and errors caused by imperfections in the orientation and leveling of the instrument. In the NOVAC installations, the most important geometrical error, the plume height uncertainty, is to a high degree minimized by arranging so that the plume can be simultaneously scanned from two different locations.

7.3. Radiative Transfer Related Error

[66] The measurement principle is based on the idea that solar light, scattered by molecules and particles in the air behind the plume, passes through the plume and is detected by the instrument. If the plume contains considerable amounts of ash, condensed water, or other particles, multiple scattering may occur in the plume, giving an extended effective path length in the plume. This leads to an overestimation of the amount of SO₂ in the plume. Also, especially under hazy conditions, light that has not passed through the plume may be scattered into the field of view of the instrument between the plume and the instrument, thus effectively "diluting" the measured absorption signal and causing an underestimation of the amount of SO₂ in the plume. These effects, which can easily give substantial errors, are well known from work using COSPEC [Millan, 1980], and likewise affect measurements using DOAS [Mori *et al.*, 2006]. In the NOVAC installations, these effects are minimized by careful selection of sites and measurement geometries. Problems with enhanced path length in the plume are minimized by avoiding the regime in which the plume condensates, and the distance between instrument and plume is significantly reduced by applying the conical scanning approach, which in turn reduces the effect of scattering below the plume.

[67] Next, to the efforts being made to avoid multiple scattering and dilution effects by choosing appropriate measurement geometries, an in-depth study of the radiative transfer in and around volcanic plumes was conducted, the results of which are described by Kern *et al.* [2009a]. Here, a radiative transfer model was used to simulate the optical paths between the Sun and a passive remote sensing instrument for a variety of volcanic measurement geometries and environmental conditions. The results show that

Table 3. Estimate of the Contribution From Different Sources to the Total Error in the Gas Flux Measurements Using NOVAC Instruments

Error Condition	Spectroscopy	Atmospheric Scattering	Measurement Geometry	Wind Speed	Total
Good	10%	10%	10%	20%	26%
Fair	15%	30%	30%	30%	54%

the errors related to an inaccurate knowledge of radiative transfer can be significant and largely depend on the distance between the plume and the instrument, the plume SO₂ concentration, the plume aerosol load, as well as aerosol conditions in the ambient atmosphere. However, a method for retrieving optical path lengths in volcanic plumes was developed. Using this method, the radiative transfer conditions can be constrained on the basis of information inherently available in the DOAS measurement spectrum. Details of this method are given by Kern *et al.* [2009a].

7.4. Wind Speed Related Error

[68] In the flux calculation the integrated number of molecules in a cross section of the plume perpendicular to the propagation direction is multiplied with the wind speed at plume height. Ideally, the concentration in each point of the cross section should be multiplied with the wind component in that point. As a compromise, the average wind speed at the average plume height is used. There are several different ways to obtain this parameter.

[69] 1. The wind can be measured at the summit of the actual volcano or at a nearby mountain. However, owing to the disturbance of the wind field by the volcano, the wind at the summit is not a good representation of the wind a few kilometers downwind from the summit where the measurement is performed.

[70] 2. Regional wind may be obtained from global models such as those provided by the European Centre for Medium-Range Weather Forecasts (ECMWF) or the National Oceanic and Atmospheric Administration (NOAA). These models are constrained by data from regular balloon launches at major airports worldwide and provide a good representation of average regional winds. However, these data do not take into account the disturbances from local topography, which may be substantial downwind of a major volcano.

[71] 3. A mesoscale model can model the topographical impact on a regional wind field to some extent and thereby improve the wind information downwind of the volcano.

[72] 4. The plume speed may be measured using a dual-beam DOAS technique as described in section 3.2. This method is, however, only useful when at least part of the plume is over the instrument. The errors associated with this type of measurement are equivalent to those found in dual-spectrometer methods with separated instruments [see McGonigle *et al.*, 2005; Williams-Jones *et al.*, 2006].

[73] In the NOVAC network, the present strategy is to use wind from global models, complemented and validated with dual-beam measurements whenever feasible. In the future, a mesoscale model, individually tailored to each volcano, will be implemented to improve the modeled wind field downwind of the volcano.

7.5. Estimate of Total Error

[74] In Table 3, an estimate of the contribution to the error budget from the different sources is given. These numbers are based on the present experience of the authors and should be regarded only as preliminary. As the errors strongly depend on local geometrical and meteorological conditions, two cases are presented. Condition “Good” means clear sky or only high uniform clouds, moderate stable winds, no haze, and good passive temperature stability of the spectrometer. “Fair” means less ideal conditions but still no low clouds, strong haze, or rain. In bad conditions with a lot of haze or rain and strongly fluctuating wind direction, the errors may easily exceed 100%. Each of the given error sources are subject to further detailed studies, and a more rigorous estimate will be possible when the results from these studies are available.

8. Installation Example

[75] During the first 3.5 years of the NOVAC project (2005–2009), gas-monitoring networks were installed on 18 volcanoes around the world, comprising in total 41 NOVAC Version I instruments and 5 NOVAC Version II instruments. These volcanoes are associated with different tectonic settings and present dissimilar levels and styles of volcanism. The logistical conditions related to the implementation of surveillance systems on these volcanoes also vary considerably, as do the risk circumstances encountered on each of them. The strategies used for installing the instruments within the project have therefore also been diverse, adapted to every particular case. As an example of these efforts, we here present the work carried out at Tungurahua volcano (Ecuador).

[76] Tungurahua (01°28′S, 78°27′W; 5023 m above sea level, asl) is a high andesitic stratocone located in the Eastern Cordillera of the Ecuadorian Andes, close to the Amazon Basin. It has presented at least one eruptive cycle per century since the thirteenth century [Le Penne *et al.*, 2008], five of them during historical times (since 1534), including the last eruptive period initiated in 1999. This eruption has been characterized by a predominant quiescent degassing style, altered by episodes of explosive events of Strombolian/Vulcanian to Subplinian nature [Arellano *et al.*, 2008]. The volcanic activity is a threat to ~25,000 inhabitants in the zone, as well as to important tourist and farming industries and two national hydroelectrical projects.

[77] Tungurahua has been monitored since 1988 by Instituto Geofísico de la Escuela Politécnica Nacional (IGEPN). Gas measurements have proven very useful for understanding the eruptive mechanisms of this volcano, and they are mainly done by remote sensing techniques (COSPEC, DOAS, FTIR, and OMI [Arellano *et al.*, 2008]) as a consequence of the logistical conditions that preclude the regular usage of, for instance, direct gas sampling.

[78] The plume emitted by Tungurahua typically drifts to the west at altitudes close to the volcano summit (90% between 230° and 290°, at 4000–5700 m asl). The high humidity that comes from the nearby jungle produces persistent cloudiness in the zone, which along with the frequent emission of volcanic ash, constitutes a major difficulty for the gas measurements. The volcano is sur-

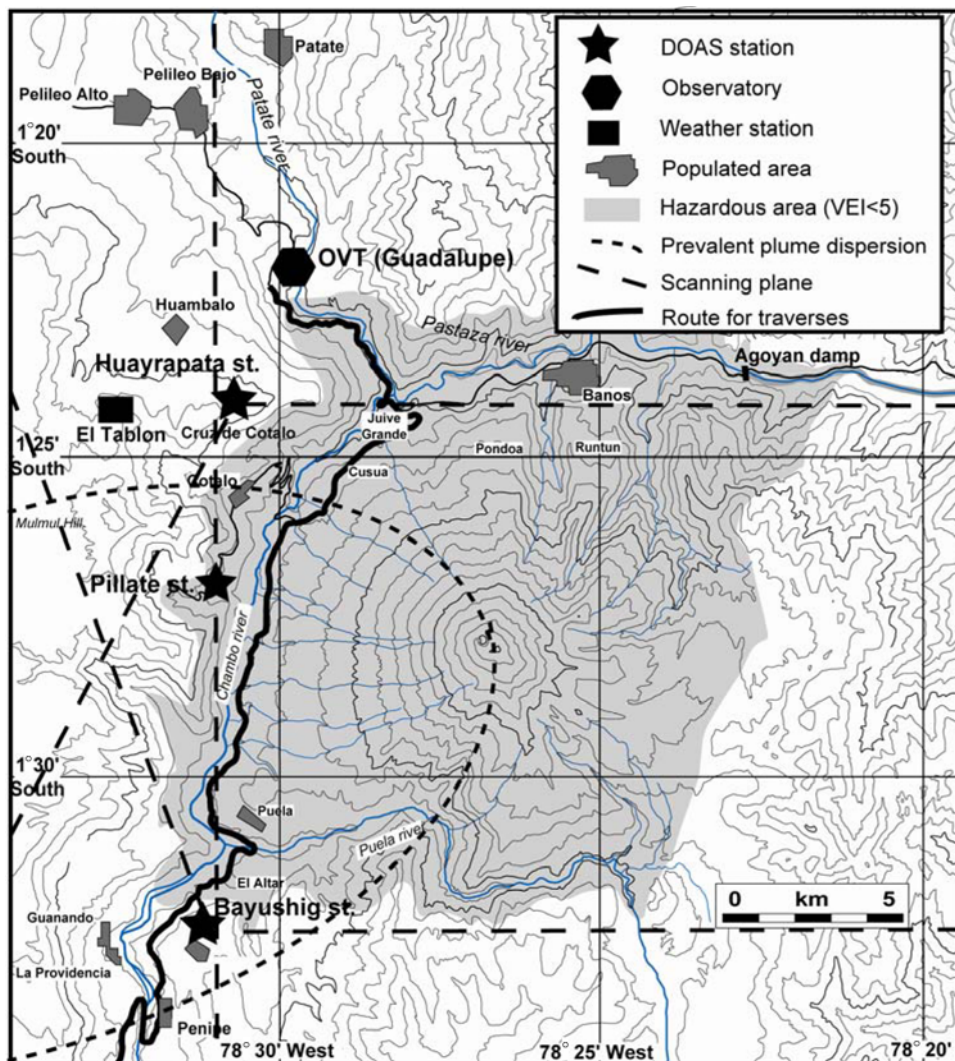


Figure 12. Installation sites and scanning directions of the NOVAC instruments at Tungurahua volcano. OVT, Tungurahua volcano observatory.

rounded by two river valleys, and its 14 km of basal diameter means that a well-distributed monitoring network around the volcano must necessarily be integrated by fairly remote stations (~10 km apart).

[79] Two NOVAC Version I instruments with conical scanning were installed in the sites Huayrapata (9.1 km, NW of the crater) and Bayushig (11.9 km, SW of the crater) in March 2007. The network in Tungurahua was complemented by the installation of a third Version I, dual-beam flat scanner in Pillate (8 km, west of the crater) in October 2007. Finally, a Version II system was deployed at Huayrapata in November 2008. This site has a 4.7 km direct line of sight to the Tungurahua volcano observatory (OVT), and it is used as a repeater site for data transmission from the other two, more remote stations. Data communication is performed by a multipoint configuration of radio modems, and power is supplied by solar panel-supported batteries, even though two of the three sites are provided with electrical energy. The stations are easily accessible and regularly visited and maintained by the staff of OVT and local farmers. Figure 12 and Table 4 show the locations and scanning directions of the NOVAC stations at Tungurahua

volcano, whereas Figure 13 is a picture of the NOVAC Version I instrument installed in Pillate.

[80] The NOVAC dual-beam instrument can only perform plume speed measurements by the autocorrelation method if certain conditions are fulfilled. These conditions pertain to the gas burden (column density greater than a threshold value, usually 50 ppm) and the direction of the plume (it must be stable for a given period of time between an angular range above the zenith position of the scanner of typically

Table 4. Geographical Information and Types of NOVAC Stations Installed at Tungurahua Volcano in Ecuador

Site	Latitude (deg)	Longitude (deg)	Altitude (m asl)	Scanning Geometry
Huayrapata	-1.404721	-78.494783	2910	Version I conic (north and west sides), Version II (variable direction)
Bayushig	-1.543496	-78.517181	2783	Version I conic (south and west sides)
Pillate	-1.453580	-78.513051	2609	Version I flat (west side)



Figure 13. NOVAC installation at Pillate station. The optical scanner is mounted on top of a pole. Electrical cables and optical fiber are fed inside the pole to a box buried under ground, which contains spectrometer and electronics. This arrangement reduces the temperature variations in the spectrometer and electronics. Also seen are the solar panel and antenna for radio transmission, as well as a dog.

$\pm 30^\circ$). In the case of the Version II instrument installed at Tungurahua volcano (Pillate site), the range of plume directions that can be used for dual-beam measurements is 240° – 300° , which is the prevalent range of wind direction in this zone ($>70\%$ of time). Plume speed measurements obtained by this method are preferred for flux calculation. If they are not available, wind information provided by the Washington Volcanic Ash Advisory Center (NOAA) or the local civil aviation service is used alternatively. Experience suggests that wind speed uncertainty is usually the largest contribution to the error budget (see Table 3), as the variations of wind regimes can be large around volcanic environments even at the time scale of scanning measurements.

[81] A comparison between the values provided by the different sources of meteorological information is not straightforward, since those usually correspond to different time and altitude frames. Such analysis is beyond the scope of this paper (see section 7.4).

[82] Geometrical conditions related to the gas flux measurement of volcanic plumes are usually complex and rapidly changing, especially close to the vent. For instance, plume bifurcation caused by crosswinds [Ernst *et al.*, 1994] or anomalous drifting occasioned by irregular wind fields make difficult the interpretation of scanning measurement results, if a simple dispersion model or plume geometry is assumed. To account for this problem, quality assessment of the plume geometry is implemented in the NOVAC program. The software assesses whether each scan is able or not to capture the entire extent of the gas plume, by using the derived slant column densities in the directions closest to the horizon and the maximum column in the entire scan. The program for flux calculation discards the measurements that show incomplete coverage of the plume. In addition, the plume center of mass, its height, and the angular range within which it is detected over a scan are calculated, providing detailed information about the geometrical conditions of the plume. From the angular range and height of the plume, in situations when the scanner detects the plume boundaries, a horizontal extension or “width” of the plume can be calculated for simple geometry, and hereby, diffusion coefficients can be derived in the context of an assumed plume dispersion model (e.g., the Gaussian diffusion model described by Arellano *et al.* [2008]).

[83] We plan to implement automatic categorization of measurement conditions in the evaluation of scans for all the NOVAC stations. Besides the above mentioned geometrical factors, scattering effects are also of high importance [Kern *et al.*, 2009a]. An empirical “quality factor” depending primarily on the estimated distance to the plume and overall level of cloudiness has been used for previous gas studies on Tungurahua volcano [Arellano *et al.*, 2008].

[84] A typical volcanic plume-scanning network is deployed in such a way that the actual time of plume observation should be as long as possible. In practice, logistical constraints such as accessibility or security determine the location of the scanners. The scanning paths are defined to expand the spatial coverage of the plume, but concurrence of scanning directions is desirable to better constrain the plume geometry, with the possibility of tomographic observation of the gas distribution inside the plume [Johansson *et al.*, 2009b]. A comparison between simultaneous observations of the same plume by two scanners is thus only possible when the plume direction intercepts the scanning paths of both instruments at the same time. It is known that atmospheric scattering effects may produce variable effects on the flux calculation of volcanic plumes. Noticeably, the distance between the scanner and the plume and the type and amount of scatterers in between determine that different instruments report different fluxes [Mori *et al.*, 2006]. For example, in the case of Tungurahua volcano, the wind direction regime determines that the Pillate station usually be closer to the plume than are the others. Consequently, the fluxes calculated from the observations of this station are usually higher than those calculated from the other stations data, if scat-

Table 5. Average Values of Statistics for the Operation of the NOVAC Stations at Tungurahua

	Huayrapata Version I	Bayushig Version I	Pillate Version I	Huayrapata Version II
Installation date	17 Mar 2007	23 Mar 2007	25 Oct 2007	20 Nov 2008
SO ₂ emission rate ^a (kg/s)	8.1 ± 3.1	8.6 ± 3.6	10.5 ± 4.5	11.3 ± 5.0
Number of daily valid scans ^b	41 ± 35	53 ± 67	54 ± 55	12 ± 10
Number of days with observations ^c	421	513	321	23

^aValues correspond to mean ± 1 standard deviation, where applicable.

^bA valid scan is a scan that provides a flux measurement by fulfilling a number of conditions concerning the column amounts, detection of plume edges, etc.

^cUntil 31 October 2008.

tering effects' corrections are not included. NOVAC is working on developing methods to estimate and, possibly, correct for these effects [Kern *et al.*, 2009a]. In the meantime, the observatories followed different routines to report the calculated gas flux that is most representative of the true volcanic emission.

[85] At IGEPN, the criterion has been to select the higher flux among those calculated from the observations of the stations that scan simultaneously the same plume. This is justified by the fact that underestimation of column densities

by scattering along the instrument-plume distance is the dominant effect for the conditions of Tungurahua volcano. If plume bifurcation occurs, which is determined from the estimated plume directions, the addition of the fluxes calculated for the different portions of the plume is reported.

[86] The NOVAC stations at Tungurahua have produced data for 86% of the time since their installations. In comparison with a prior scanning Mini-DOAS system in operation since July 2004 [Arellano *et al.*, 2008], the NOVAC system has more efficient power consumption,

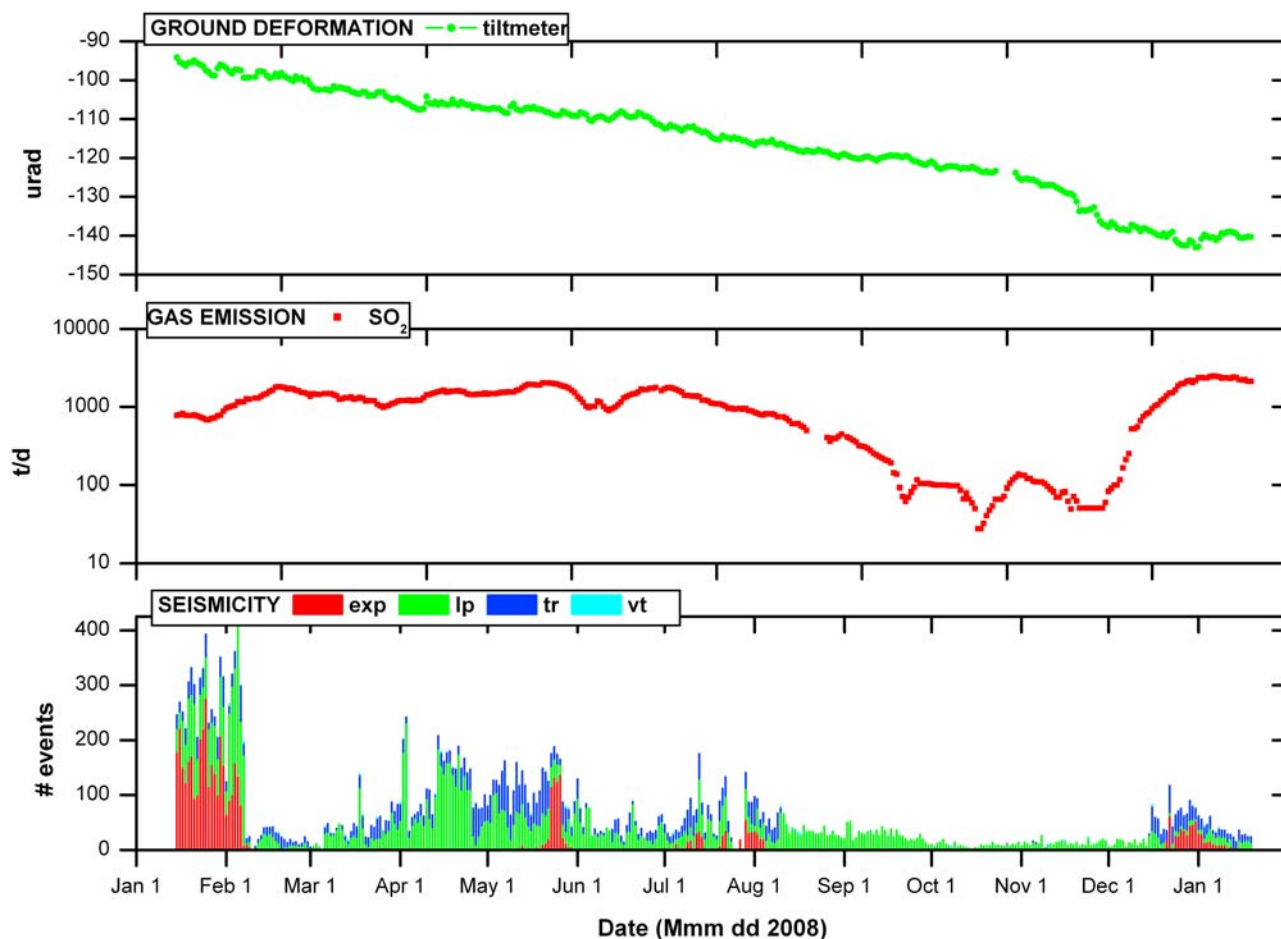


Figure 14. Results of measurements of the NOVAC stations at Tungurahua. (top) Deformation is measured in microradians by a tiltmeter located in the northern flank of the volcano. (middle) SO₂ gas emission rate is measured in tons per day by the NOVAC instruments described in this article. (bottom) Seismicity is quantified as the number of seismic events per day by a dense network of seismometers around the volcano. Seismic events are classified as explosions (exp), long-period events (lp), tremor (tr), and volcano-tectonic (vt) events. Further details about the location and type of geodetic and seismologic systems can be found at <http://www.igepn.edu.ec>.

more robust acquisition and handling of data, and easier and more accurate data analysis. Adverse weather conditions are the most important source of uncertainty in the measurements at Tungurahua; however, the spatial distribution of the stations, which guarantees plume coverage during 90% of the time, not only improves significantly the time-resolved determination of plume height and direction but also offers clues into some radiative transfer effects by allowing simultaneous studying of the plume from varying distances (see section 7.3). The measurements of the plume width at Tungurahua are also being used to estimate the diffusion coefficients of SO₂ in the atmosphere, with the help of which time and height profiles can be calculated, with the further purpose of validating atmospheric dispersion models and better assessing the environmental impact of the emissions of volcanic gas and ash. Table 5 compiles some aspects of the performance of the NOVAC stations.

[87] It is noteworthy in Table 5 that average values of different variables are not identical for the four stations. This is primarily caused by the different operation periods of the instruments; however, it also reflects the effect of the local conditions (e.g., cloudiness or distance to the plume) over the measurements. From the volcanologist's perspective, it is thus important to evaluate which station provides the more reliable results during a certain period of time. Taking these criteria into account, the mean SO₂ emission rate of Tungurahua during March 2007 to December 2008 measured by NOVAC amounts to 9.3 ± 3.7 ($\pm 1\sigma$) kg/s. Although during this period, passive degassing predominated, important explosive episodes occurred in September–October 2007, November 2007 to February 2008, May 2008, and December 2008. During these eruptions, fluxes as high as 60 kg/s were observed, in clear correspondence with the increase in the intensity of other geophysical parameters monitored by IGEPN (see Figure 14).

9. Discussions

[88] The NOVAC project is aimed at establishing a global network of instruments for volcanic gas emission monitoring with the purpose of improving the risk assessment of active volcanoes. This article has presented the instrument design, network architecture, and emission measurement strategies of the NOVAC global volcanic-gas-monitoring network. The two instrument versions used are presented, as well as the flat and conical scanning geometries. Autonomous instruments and automatic derivation of the SO₂ columns and fluxes can reduce the workload on the observatories and provide valuable information in case of a volcanic crisis. The wireless data communication to the instruments and connection to the Internet enable automatic and continuous uploading of spectrum files and evaluation results to the central ftp and database servers.

[89] A total of 46 instruments have so far been installed at 18 volcanoes worldwide, producing time series of gas emissions over several months/years since installation. The robustness and scalability of the network will be examined over the long term. The main error sources of the measurements will be studied in detail during the scope of the NOVAC project, and the results will be used in more automatic quality control routines.

[90] As the amount of collected data increases, correlation studies with other geophysical data will be conducted aimed at increasing understanding of the geophysical and geochemical behavior of the volcanoes and thereby improving risk assessment. In addition, in the following years the data will also be exploited for global estimates of volcanic gas emissions, studies of tropospheric and stratospheric atmospheric chemistry, and ground-based validation of satellites.

[91] **Acknowledgments.** This project was funded by the European Commission Framework 6 Research Program. Additional support from the Swedish International Development Cooperation Agency is greatly appreciated.

References

- Arellano, S., M. Hall, P. Samaniego, J.-L. Le Penec, A. Ruiz, I. Molina, and H. Yepes (2008), Degassing patterns of Tungurahua volcano (Ecuador) during the 1999–2006 eruptive period, inferred from remote spectroscopic measurements of SO₂ emissions, *J. Volcanol. Geotherm. Res.*, *176*, 151–162, doi:10.1016/j.jvolgeores.2008.07.007.
- Baxter, P. (1990), Medical effects of volcanic eruptions, *Bull. Volcanol.*, *52*, 532–544, doi:10.1007/BF00301534.
- Bobrowski, N., G. Hönninger, U. Platt, and B. Galle (2003), Detection of bromine monoxide in a volcanic plume, *Nature*, *423*(6937), 273–276, doi:10.1038/nature01625.
- Burton, M., T. Caltabiano, G. Salerno, F. Mure, and D. Condarelli (2004), Automatic measurements of SO₂ flux on Stromboli and Mt. Etna using a network of scanning UV spectrometers, *Geophys. Res. Abstr.*, *6*, Abstract EGU04-A-03970.
- Delmelle, P., J. Stix, P. Baxter, J. Garcia-Alvarez, and J. Barquero (2002), Atmospheric dispersion, environmental effects and potential health hazard associated with the low-altitude gas plume of Masaya volcano, Nicaragua, *Bull. Volcanol.*, *64*, 423–434, doi:10.1007/s00445-002-0221-6.
- Edmonds, M., C. Oppenheimer, D. M. Pyle, R. A. Herd, and G. Thompson (2003a), SO₂ emissions from Soufrière Hills Volcano and their relationship to conduit permeability, hydrothermal interaction and degassing regime, *J. Volcanol. Geotherm. Res.*, *124*, 23–43, doi:10.1016/S0377-0273(03)00041-6.
- Edmonds, M., R. A. Herd, B. Galle, and C. M. Oppenheimer (2003b), Automated, high time resolution measurements of SO₂ flux at Soufrière Hills Volcano, Montserrat, *Bull. Volcanol.*, *65*, 578–586, doi:10.1007/s00445-003-0286-x.
- Ernst, G., P. Davies, and R. S. J. Sparks (1994), Bifurcation of volcanic plumes in a crosswind, *Bull. Volcanol.*, *56*, 159–169, doi:10.1007/BF00279601.
- Friess, U., P. S. Monks, J. J. Remedios, A. Rozanov, R. Sinreich, T. Wagner, and U. Platt (2006), MAX-DOAS O₄ measurements: A new technique to derive information on atmospheric aerosols: 2. Modeling studies, *J. Geophys. Res.*, *111*, D14203, doi:10.1029/2005JD006618.
- Galle, B. (2007), Method and device for measuring emissions of gaseous substances to the atmosphere using scattered sunlight spectroscopy, Patent PCT/SE/2006/000738, U.S. Patent and Trademark Off., Washington, D. C.
- Galle, B., C. Oppenheimer, A. Geyer, A. McGonigle, M. Edmonds, and L. Horrocks (2003), A miniaturised ultraviolet spectrometer for remote sensing of SO₂ fluxes: A new tool for volcano surveillance, *J. Volcanol. Geotherm. Res.*, *119*, 241–254.
- Galle, B., U. Platt, C. Oppenheimer, M. Millan, L. Alonso, and D. Chen (2006), Final scientific report on EU-Project DORSIVA, *Rep. 26051*, Chalmers Univ. of Technol., Gothenburg, Sweden.
- Halmer, M. M., H.-U. Schmincke, and H.-F. Graf (2002), The annual volcanic gas input into the atmosphere, in particular into the stratosphere: A global data set for the past 100 years, *J. Volcanol. Geotherm. Res.*, *115*, 511–528, doi:10.1016/S0377-0273(01)00318-3.
- Hartl, A., B. C. Song, and I. Pundt (2006), 2-D reconstruction of atmospheric concentration peaks from horizontal long path DOAS tomographic measurements: Parameterisation and geometry within a discrete approach, *Atmos. Chem. Phys.*, *6*, 847–861.
- Heckel, A., A. Richter, T. Tarsu, F. Wittrock, C. Hak, I. Pundt, W. Junkermann, and J. P. Burrows (2005), MAX-DOAS measurements of formaldehyde in the Po-Valley, *Atmos. Chem. Phys.*, *5*, 909–918.
- Hoff, R. M. (1992), Differential SO₂ column measurements of the Mt. Pinatubo volcanic plume, *Geophys. Res. Lett.*, *19*(2), 175–178, doi:10.1029/91GL02793.
- Hoff, R. M., and M. M. Millan (1981), Remote SO₂ mass flux measurements using Cospec, *J. Air Pollut. Control Assoc.*, *31*(4), 381–384.

- Hönninger, G., and U. Platt (2002), Observations of BrO and its vertical distribution during surface ozone depletion at Alert, *Atmos. Environ.*, 36(15–16), 2481–2489, doi:10.1016/S1352-2310(02)00104-8.
- Hönninger, G., C. von Friedeburg, and U. Platt (2004), Multi axis differential optical absorption spectroscopy (MAX-DOAS), *Atmos. Chem. Phys.*, 4, 231–254.
- Intergovernmental Panel on Climate Change (2007), *Climate Change 2007: The Physical Science Basis, Contribution of Working Group I to the Fourth Assessment Report of the Intergovernmental Panel on Climate Change*, Cambridge Univ. Press, New York.
- Johansson, M. (2008), Geometrical errors in flux measurements using the NOVAC scanning DOAS instrument, paper presented at Fourth International DOAS Workshop, Accent Project, Hefei, China.
- Johansson, M., B. Galle, Y. Zhang, C. Rivera, D. Chen, and K. Wyser (2009a), The dual-beam mini-DOAS technique: Measurements of volcanic gas emission, plume height and plume speed with a single instrument, *Bull. Volcanol.*, 71, 747–751, doi:10.1007/s00445-008-0260-8.
- Johansson, M., B. Galle, C. Rivera, and Y. Zhang (2009b), Tomographic reconstruction of gas plumes using scanning DOAS, *Bull. Volcanol.*, 71, 1169–1178, doi:10.1007/s00445-009-0292-8.
- Kazahaya, R., T. Mori, K. Kazahaya, and J. Hirabayashi (2008), Computed tomography reconstruction of SO₂ concentration distribution in the volcanic plume of Miyakejima, Japan, by airborne traverse technique using three UV spectrometers, *Geophys. Res. Lett.*, 35, L13816, doi:10.1029/2008GL034177.
- Kern, C. (2009), Spectroscopic measurements of volcanic gas emissions in the ultra-violet wavelength region, Ph.D. thesis, Univ. of Heidelberg, Heidelberg, Germany.
- Kern, C., T. Deutschmann, A. Vogel, M. Wöhrbach, T. Wagner, and U. Platt (2009a), Radiative transfer corrections for accurate spectroscopic measurements of volcanic gas emissions, *Bull. Volcanol.*, doi:10.1007/s00445-009-0313-7, in press.
- Kern, C., H. Sihler, L. Vogel, C. Rivera, M. Herrera, and U. Platt (2009b), Halogen oxide measurements at Masaya Volcano, Nicaragua using active long path differential optical absorption spectroscopy, *Bull. Volcanol.*, 71, 659–670, doi:10.1007/s00445-008-0252-8.
- Le Penneç, J.-L., D. Jaya, P. Samaniego, P. Ramón, S. Moreno Yáñez, J. Eged, and J. van der Plicht (2008), The AD 1300–1700 eruptive periods at Tungurahua volcano, Ecuador, revealed by historical narratives, stratigraphy and radiocarbon dating, *J. Volcanol. Geotherm. Res.*, 176, 70–81.
- McGonigle, A. J. S., D. R. Hilton, T. P. Fischer, and C. Oppenheimer (2005), Plume velocity determination for volcanic SO₂ flux measurements, *Geophys. Res. Lett.*, 32, L11302, doi:10.1029/2006GL022470.
- Millan, M. M. (1980), Remote sensing of air pollutants: A study of some atmospheric scattering effects, *Atmos. Environ.*, 14(11), 1241–1253.
- Moffat, A. J., and M. M. Millan (1971), The applications of optical correlation techniques to the remote sensing of SO₂ plumes using sky light, *Atmos. Environ.*, 5(8), 677–690.
- Mori, T., K. Kazahaya, M. Ohwada, J. Hirabayashi, and S. Yoshikawa (2006), Effect of UV scattering on SO₂ emission rate measurements, *Geophys. Res. Lett.*, 33, L17513, doi:10.1029/2006GL026285.
- Noxon, J. F. (1975), Nitrogen-dioxide in stratosphere and troposphere measured by ground-based absorption spectroscopy, *Science*, 189(4202), 547–549.
- Olmos, R., et al. (2007), Anomalous emissions of SO₂ during the recent eruption of Santa Ana volcano, El Salvador, Central America, *Pure Appl. Geophys.*, 164(12), 2489–2506.
- Platt, U., D. Perner, and H. W. Pätz (1979), Simultaneous measurement of atmospheric CH₂O, O₃ and NO₂ by differential optical absorption, *J. Geophys. Res.*, 84, 6329–6335.
- Robock, A. (2002), Pinatubo eruption: The climatic aftermath, *Science*, 295(5558), 1242–1244.
- Salerno, G., M. Burton, T. Caltabiano, B. N. Bruno, D. Condarelli, L. V. Longo, and M. F. Mure (2006), High-term resolution SO₂ flux measurements using an automated UV scanner array: First 16-month results on Mt. Etna (Italy), *Geophys. Res. Abstr.*, 8, Abstract EGU06-A-03098.
- Salerno, G., M. Burton, C. Oppenheimer, T. Caltabiano, D. Randazzo, N. Bruno, and V. Longo (2009), Three-years of SO₂ flux measurements of Mt. Etna using an automated UV scanner array: Comparison with conventional traverses and uncertainties in flux retrieval, *J. Volcanol. Geotherm. Res.*, 183, 76–83.
- Sinreich, R., U. Friess, T. Wagner, and U. Platt (2005), Multi axis differential optical absorption spectroscopy (MAXDOAS) of gas and aerosol distributions, *Faraday Discuss.*, 130, 132–164.
- Solomon, S., A. L. Schmeltekopf, and R. W. Sanders (1987), On the interpretation of zenith sky absorption measurements, *J. Geophys. Res.*, 92, 8311–8319.
- Sommer, T. (2008), Direct sun light measurements of volcanic plumes using differential optical absorption spectroscopy, Diploma thesis, Univ. of Heidelberg, Heidelberg, Germany.
- Sparks, R. S. J. (2003), Dynamics of magma degassing, in *Volcanic Degassing*, edited by C. Oppenheimer, D. Pyle, and J. Barclay, *Geol. Soc. Spec. Publ.*, 213, 5–22.
- Stoiber, R. E., L. L. Malinconico, and S. N. Williams (1983), Use of the correlation spectrometer at volcanoes, in *Forecasting Volcanic Events*, edited by H. Tazieff and J. C. Sabroux, pp. 425–444, Elsevier, Amsterdam.
- Stutz, J., and U. Platt (1996), Numerical analysis and estimation of the statistical error of differential optical absorption spectroscopy measurements with least-squares methods, *Appl. Opt.*, 35(30), 6041–6053.
- Symonds, R. B., W. I. Rose, G. J. S. Bluth, and T. M. Gerlach (1994), Volcanic-gas studies: Methods, results, and applications, *Rev. Mineral. Geochem.*, 30(1), 1–66.
- Vandaele, A. C., P. C. Simon, J. M. Guilmet, M. Carleer, and R. Colin (1994), SO₂ absorption cross-section measurement in the UV using a Fourier-transform spectrometer, *J. Geophys. Res.*, 99, 25,599–25,605.
- Voigt, S., J. Orphal, K. Bogumil, and J. P. Burrows (2001), The temperature dependence (203–293 K) of the absorption cross sections of O₃ in the 230–850 nm region measured by Fourier-transform spectroscopy, *J. Photochem. Photobiol. A*, 143(1), 1–9.
- Volkamer, R., T. Eitzkorn, A. Geyer, and U. Platt (1998), Correction of the oxygen interference with UV spectroscopic (DOAS) measurements of monocyclic aromatic hydrocarbons in the atmosphere, *Atmos. Environ.*, 32(21), 3731–3747.
- Wagner, T., B. Dix, C. V. Friedeburg, U. Frieß, S. Sanghavi, R. Sinreich, and U. Platt (2004), MAX-DOAS O₄ measurements: A new technique to derive information on atmospheric aerosols—Principles and information content, *J. Geophys. Res.*, 109, D22205, doi:10.1029/2004JD004904.
- Williams-Jones, G., K. A. Horton, T. Elias, H. Garbeil, P. J. Mougini-Mark, A. J. Sutton, and A. J. L. Harris (2006), Accurately measuring volcanic plume velocity with multiple UV spectrometers, *Bull. Volcanol.*, 68, 328–332.
- Wright, T. E., M. Burton, D. M. Pyle, and T. Caltabiano (2008), Scanning tomography of SO₂ distribution in a volcanic gas plume, *Geophys. Res. Lett.*, 35, L17811, doi:10.1029/2008GL034640.
- Yu, Y., A. Geyer, B. Galle, L. Chen, P. Xie, and U. Platt (2004), Observations of carbon disulfide by differential optical absorption spectroscopy in Shanghai, *Geophys. Res. Lett.*, 31, L11107, doi:10.1029/2004GL019543.

S. Arellano, B. Galle, M. Johansson, C. Rivera, and Y. Zhang, Department of Radio and Space Science, Chalmers University of Technology, Hörsalsvagen 11, S-41296 Gothenburg, Sweden. (bo.galle@chalmers.se)

S. Hidalgo, Instituto Geofísico de la Escuela Politécnica Nacional, Ladrón de Guevara E11-253, Apartado 2759, Quito, Ecuador.

C. Kern, T. Lehmann, and U. Platt, Institute for Environmental Physics, University of Heidelberg, D-69120 Heidelberg, Germany.

M. Kihlman, Kihlman El och Data Utveckling, S-41457 Gothenburg, Sweden.